nature biotechnology

Microscale culture of human liver cells for drug development

Salman R Khetani[1] & Sangeeta N Bhatia[1,2]

Tissue function depends on hierarchical structures extending from single cells (∼10 μm) to functional subunits (100 μm–1 mm) that coordinate organ functions. Conventional cell culture disperses tissues into single cells while neglecting higher-order processes. The application of semiconductor-driven microtechnology in the biomedical arena now allows fabrication of microscale tissue subunits that may be functionally improved[1] and have the advantages of miniaturization[2]. Here we present a miniaturized, multiwell culture system for human liver cells with optimized microscale architecture that maintains phenotypic functions for several weeks. The need for such models is underscored by the high rate of pre-launch and post-market attrition of pharmaceuticals due to liver toxicity[3]. We demonstrate utility through assessment of gene expression profiles, phase I/II metabolism, canalicular transport, secretion of liver-specific products and susceptibility to hepatotoxins. The combination of microtechnology and tissue engineering may enable development of integrated tissue models in the so-called 'human on a chip'[4].

Cellular functions are influenced not only by cell-autonomous programs but also by microenvironmental stimuli, which include neighboring cells, extracellular matrix, soluble factors and physical forces. To study cellular responses to distinct local stimuli, one must use tools that allow control over these inputs on the order of single-cell dimensions (∼10 μm). In semiconductor microfabrication, precision control over surface properties at such dimensions is trivial as current devices include nanometer-scale features. Over the last decade, microtechnology tools have emerged to probe biomedical phenomena at relevant length scales and to miniaturize and parallelize biomedical assays[1,2,5,6]. Here we use microtechnology to study the impact of liver-cell micropatterning on cellular function and use the findings to fabricate a multiwell-format culture system.

The liver has a central role in drug metabolism and toxicity. Drug-induced liver toxicity is the leading cause of acute liver failure and post-market drug withdrawals[3]. Preclinical animal studies are inadequate to evaluate toxicity because of species-specific variation between human and animal hepatocellular functions, necessitating supplementation of animal data with assays to assess human responses[7]. Several limited human liver models are currently used: liver slices, microsomes, cell lines and primary hepatocytes[8–12]. Although liver slices retain *in vivo* cytoarchitecture, they are viable only for ∼1 d and are not amenable to high-throughput screening. Microsomes are used in high-throughput systems to identify enzymes involved in drug metabolism[9,13], but lack the dynamic gene expression and intact cellular machinery required for toxicity testing. Although hepatocarcinoma-derived cell lines and immortalized hepatocytes can be reproducible and inexpensive, they display abnormal levels of liver-specific functions[14]. Thus, of the four models, primary hepatocytes are considered to be the best choice for ADME/Tox (absorption, distribution, metabolism and excretion/toxicity) applications because they are simple to use and their cytoarchitecture remains intact; however, hepatic functions rapidly decline under conventional culture conditions[9,11,12].

Here we describe a microtechnology-based process using elastomeric stencils to culture human liver cells in an industry-standard multiwell format. Our approach incorporates 'soft lithography' techniques, using reusable, elastomeric molds of microfabricated structures to overcome limitations of photolithography[15]. The process uses polydimethylsiloxane (PDMS) stencils consisting of 300-μm-thick membranes with through-holes at the bottom of each well in a 24-well mold (**Fig. 1a**). The multiwell mold is sealed against a polystyrene plate, collagen-I is adsorbed to exposed polystyrene, the stencil is removed and a 24-well PDMS 'blank' is applied. Selective hepatocyte adhesion to collagenous domains yields 'micropatterned' clusters, which are subsequently surrounded by mouse 3T3-J2 fibroblasts. The diameter of through-holes in stencils determines the size of collagenous domains and thereby the balance of homotypic and heterotypic interactions in microscale cultures.

We varied collagen island diameter over several orders of magnitude and observed that hepatocyte clustering improved liver-specific functions compared with unorganized cultures (**Supplementary Fig. 1** online). Furthermore, hepatocyte functions were maximal for the configuration containing ∼500-μm islands with ∼1,200-μm center-to-center spacing. These findings are consistent with our rodent data in that 3T3 fibroblasts stabilized hepatocyte functions across both species[6,16]; however, human hepatocytes were more dependent on homotypic interactions than rat hepatocytes. Thus, the system developed here uses 24-well plates with each well containing ∼10,000 hepatocytes organized in 37 colonies of 500-μm diameter and

[1]Division of Health Sciences and Technology, Department of Electrical Engineering and Computer Science, Massachusetts Institute of Technology, 77 Massachusetts Avenue, E19-502D, Cambridge, Massachusetts 02139, USA. [2]Division of Medicine, Brigham & Women's Hospital, Boston, Massachusetts 02115, USA. Correspondence should be addressed to S.N.B. (sbhatia@mit.edu).

Received 7 August; accepted 1 November; published online 18 November 2007; doi:10.1038/nbt1361

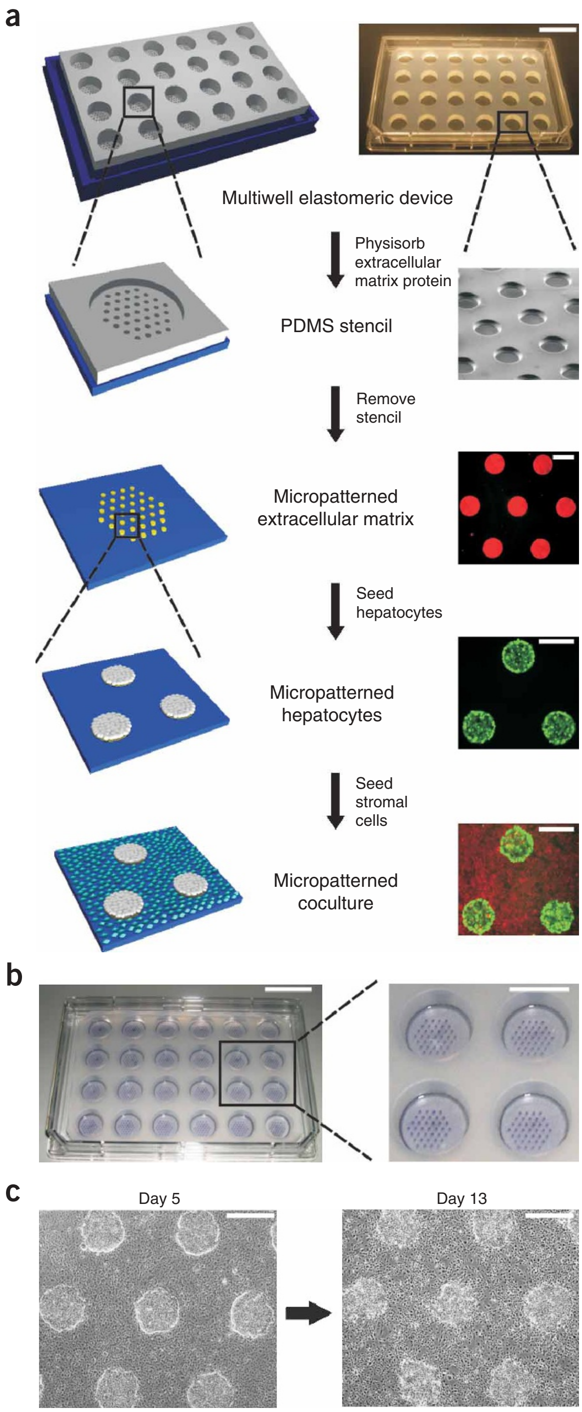

Figure 1 Soft lithographic process to fabricate microscale liver hepatocyte cultures in a multiwell format. (**a**) Schematic of the process flow aside photomicrographs taken at each step. A reusable PDMS stencil is seen consisting of membranes with through-holes at the bottom of each well in a 24-well mold. To micropattern all wells simultaneously, one seals the device under dry conditions to a culture substrate. A photograph of a device (scale bar represents 2 cm) sealed to a polystyrene omni-tray is seen along with an electron micrograph of a thin stencil membrane. Each well is incubated with a solution of extracellular matrix protein (ECM) to allow protein to adsorb to the substrate via the through-holes. The stencil is then peeled off leaving micropatterned ECM protein on the substrate (fluorescently labeled collagen pattern). A 24-well PDMS 'blank' lacking membranes is then sealed to the plate before cell seeding (not shown here). Primary hepatocytes selectively adhere to matrix-coated domains, allowing supportive stromal cells to be seeded into the remaining bare areas (hepatocytes labeled green and fibroblasts orange; scale bar is 500 μm). (**b**) Photograph of a 24-well device with repeating hepatic microstructures (37 colonies of 500-μm diameter in each well), stained purple by MTT. Scale bars, 2 cm and 1 cm for enlargement. (**c**) Phase-contrast micrographs of micropatterned cocultures. Primary human hepatocytes are spatially arranged in ~500-μm collagen-coated islands with ~1,200 μm center-to-center spacing, surrounded by 3T3-J2 fibroblasts. Images depict pattern fidelity over several weeks of culture. Scale bars, 500 μm.

surrounded by fibroblasts (micropatterned cocultures), for a total of 888 repeating hepatic microstructures per plate (**Fig. 1b**). The microscale architecture remained stable for several weeks in culture, which enabled microscopic tracking of individual islands (**Fig. 1c**).

To qualitatively assess the stability of micropatterned cocultures, we monitored hepatocyte morphology and found that it was maintained for 4–6 weeks (**Fig. 2a**). To quantitatively assess the stability of liver-specific functions in micropatterned cocultures, we measured albumin secretion and urea synthesis as surrogate markers of protein synthesis and nitrogen metabolism, respectively (**Fig. 2b**). Albumin secretion in micropatterned cocultures took ~3–6 d to reach steady-state levels, whereas urea synthesis stabilized immediately. Rapid loss of morphological features and liver-specific functions was confirmed in pure cultures[16]. To assess the utility of micropatterned cocultures for metabolism studies, we characterized cytochrome-P450 (CYP450) activity, phase II conjugation and canalicular transport. CYP450 activity in micropatterned cocultures was assessed over several weeks using fluorometric substrates for high-throughput screening and isoenzyme-specific probes requiring chromatographic separation of metabolites[13,17]. We found that activities of several CYP450s were well retained (>50% of the levels in fresh hepatocytes) for several weeks in uninduced micropatterned cocultures (**Fig. 2c**), whereas marked loss of CYP450 activities was confirmed in pure cultures. Phase II activities were also retained for several weeks in micropatterned cocultures as evaluated by conjugation of 7-hydroxycoumarin with glucuronide/sulfate moieties. Lastly, we observed canalicular transport in micropatterned cocultures following transport of a fluorometric substrate into the bile canaliculi between hepatocytes (**Fig. 2d**).

We profiled global gene expression of micropatterned cocultures over several weeks. Before extraction of hepatocyte RNA, fibroblasts were removed by selective trypsinization (~95% purity, **Supplementary Methods** online). Micropattern clustering enhances the ability to obtain purified hepatocyte RNA from cocultures and is therefore advantageous for genome-wide analyses. Expression profiles of hepatocytes from micropatterned cocultures were compared to those of all cell types of human liver after tissue disruption but before hepatocyte purification, freshly isolated purified hepatocytes in suspension and unorganized pure hepatocytes 1 week after plating. Overall, hepatocytes in micropatterned cocultures were stable for 4-6 weeks, as indicated by high expression levels of liver-specific genes relevant for evaluating drug metabolism and toxicity.

All liver-specific CYP450 (**Fig. 3a**) and phase II genes (**Fig. 3b**) found on the microarray (~91 genes) were expressed at statistically significant levels in hepatocytes from micropatterned cocultures as old as 6 weeks, long after pure hepatocytes had lost phenotypic functions (~1 week). However, levels of CYP450 transcripts in micropatterned cocultures relative to fresh hepatocytes were highly variable across different donors. Our findings are consistent with the literature[18,19], which indicates high variability of gene expression profiles in freshly isolated human hepatocytes due to factors such as drug-mediated enzyme induction in the donor, isolation procedures and storage/shipment conditions. Additionally, we confirmed reports that mRNA levels do not always correlate quantitatively with enzymatic activity[20]. Measured CYP450 activities in micropatterned cocultures and in freshly isolated human hepatocytes (**Fig. 2c**) were much more similar than CYP450 mRNA levels in the two models. We also analyzed expression levels of nuclear receptors that modulate expression of metabolism enzymes after hepatocyte exposure to xenobiotics, liver-enriched transcription factors that regulate liver-specific

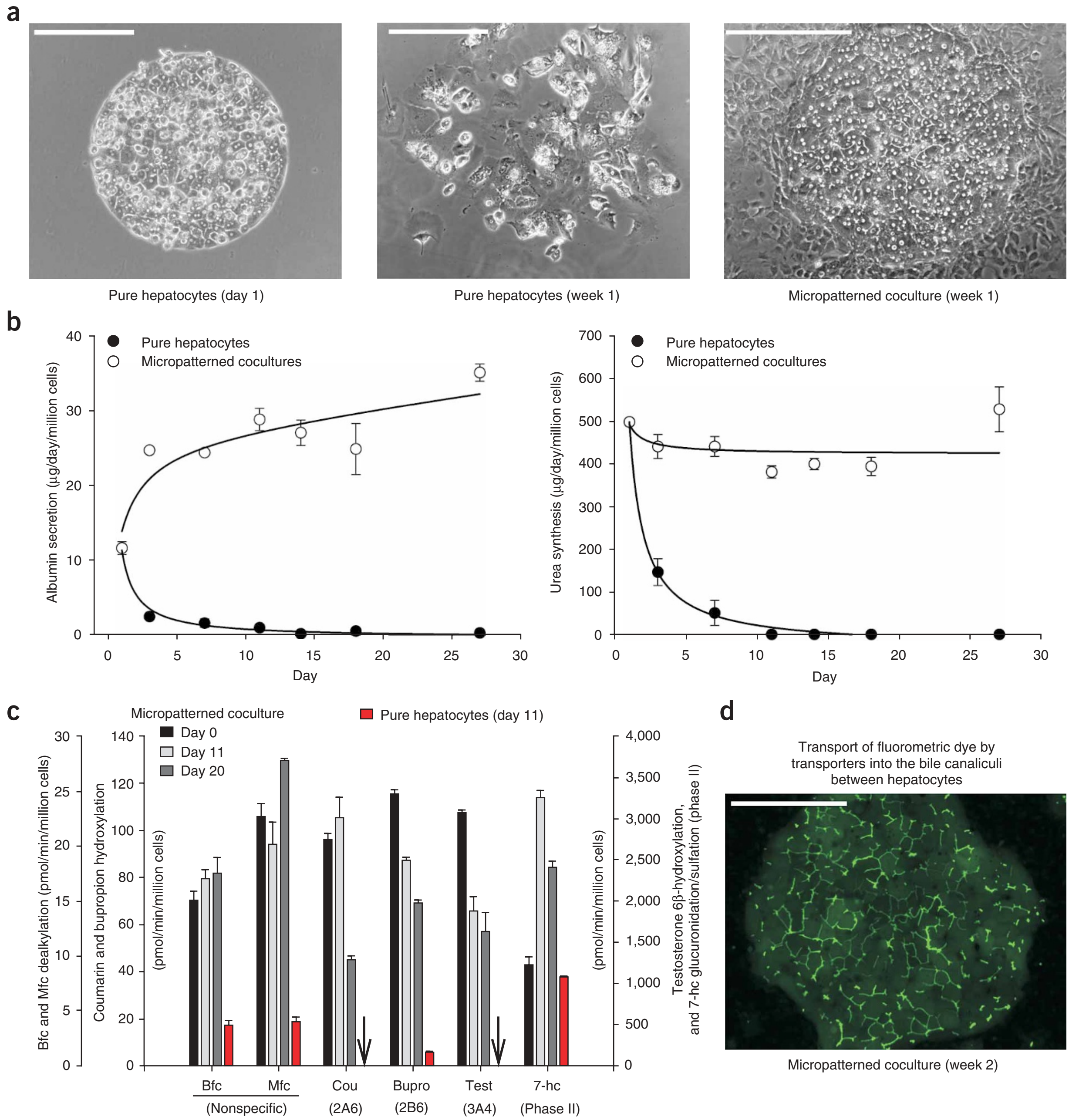

Figure 2 Functional characterization of microscale liver cultures. (**a**) Morphology of primary human hepatocytes in micropatterned cocultures over time (representative micrographs at day 1 and week 1). Morphology of pure hepatocytes at week 1 is shown for comparison. Scale bars, 250 µm. (**b**) Rates of albumin secretion and urea synthesis in micropatterned cocultures and pure hepatocyte cultures over several weeks. (**c**) Activities of phase I (CYP450) and phase II (conjugation) enzymes measured via fluorometric (Bfc, Mfc, coumarin, 7-hc) and conventional probe substrates (bupropion HCL and testosterone) in micropatterned cocultures at baseline (un-induced) over several weeks. Enzyme activities in pure hepatocytes on day 0 (6 h after plating) and day 11 are shown for comparison. Arrows pointing to the *x*-axis indicate undetectable substrate metabolism in pure hepatocytes on day 11. Specific activities of CYP 3A4, 2B6 and 2A6 were measured using testosterone 6β-hydroxylation, bupropion hydroxylation and coumarin 7-hydroxylation, respectively (see **Supplementary Methods**). Phase II activity was assessed by measuring the amount of 7-Hydroxycoumarin (7-HC) conjugated with glucuronide and sulfate groups. Mfc, 7-methoxy-4-trifluoromethylcoumarin; Bfc, 7-benzyloxy-4-trifluoromethylcoumarin; Cou, coumarin; Bupro; bupropion HCL; Test; testosterone. All error bars represent s.e.m. ($n = 3$). (**d**) Phase 3 transporter activity in micropatterned cocultures. Cultures were incubated with 5-(and-6)-carboxy-2′,7′-dichlorofluorescein diacetate, which gets internalized by hepatocytes, cleaved by intracellular esterases and excreted into the bile canaliculi between hepatocytes by transporters. Scale bar, 250 µm.

functions, and influx/efflux transporters. We found that several important genes from these classes were expressed at statistically significant levels in micropatterned cocultures as old as 6 weeks ($P < 0.05$; **Fig. 3c**). Furthermore, we confirmed marked loss of liver-specific transcripts in pure hepatocytes (week 1) compared with micropatterned cocultures and freshly isolated hepatocytes (**Fig. 3d**). Lastly, we found that the transcriptome of hepatocytes in micropatterned cocultures was relatively stable ($R^2 = 0.92$, slope $= 1.1$) when comparing weeks 1 and 3 (**Supplementary Fig. 2** online).

To assess the utility of micropatterned cocultures for toxicity screening, we quantified the acute and chronic toxicity of model hepatotoxins. Compounds were characterized by TC_{50}, the concentration that produced a 50% reduction in mitochondrial activity after acute (24 h) exposure (**Fig. 4a**). Relative toxicity corresponded to relative hepatotoxicity of these compounds in humans. For example, TC_{50} for cadmium was three orders of magnitude lower than TC_{50} values for aspirin and caffeine. When we compared compounds within the thiazolidinedione drug class, troglitazone (Rezulin; a hypoglycemic withdrawn by the FDA due to hepatotoxicity) was much more acutely toxic than its structural analogs, rosiglitazone (Avandia) and pioglitazone (Actos, Glustin), known to have a larger margin of safety and approved by the FDA[21]. Established mechanisms of toxicity could also be inferred from our toxicity profiles. For instance, cadmium showed a relatively linear toxic profile whereas acetaminophen exhibited a toxicity 'shoulder' consistent with proposed glutathione depletion[3] (**Supplementary Fig. 3** online). Next, we demonstrated dose and time-dependent chronic toxicity of troglitazone (**Fig. 4b**). Concentrations not lethal at 24 h caused extensive cell death after up to 9 d of exposure. Furthermore, severe morphologic changes in hepatocytes were readily observed, allowing detection of sublethal toxicity

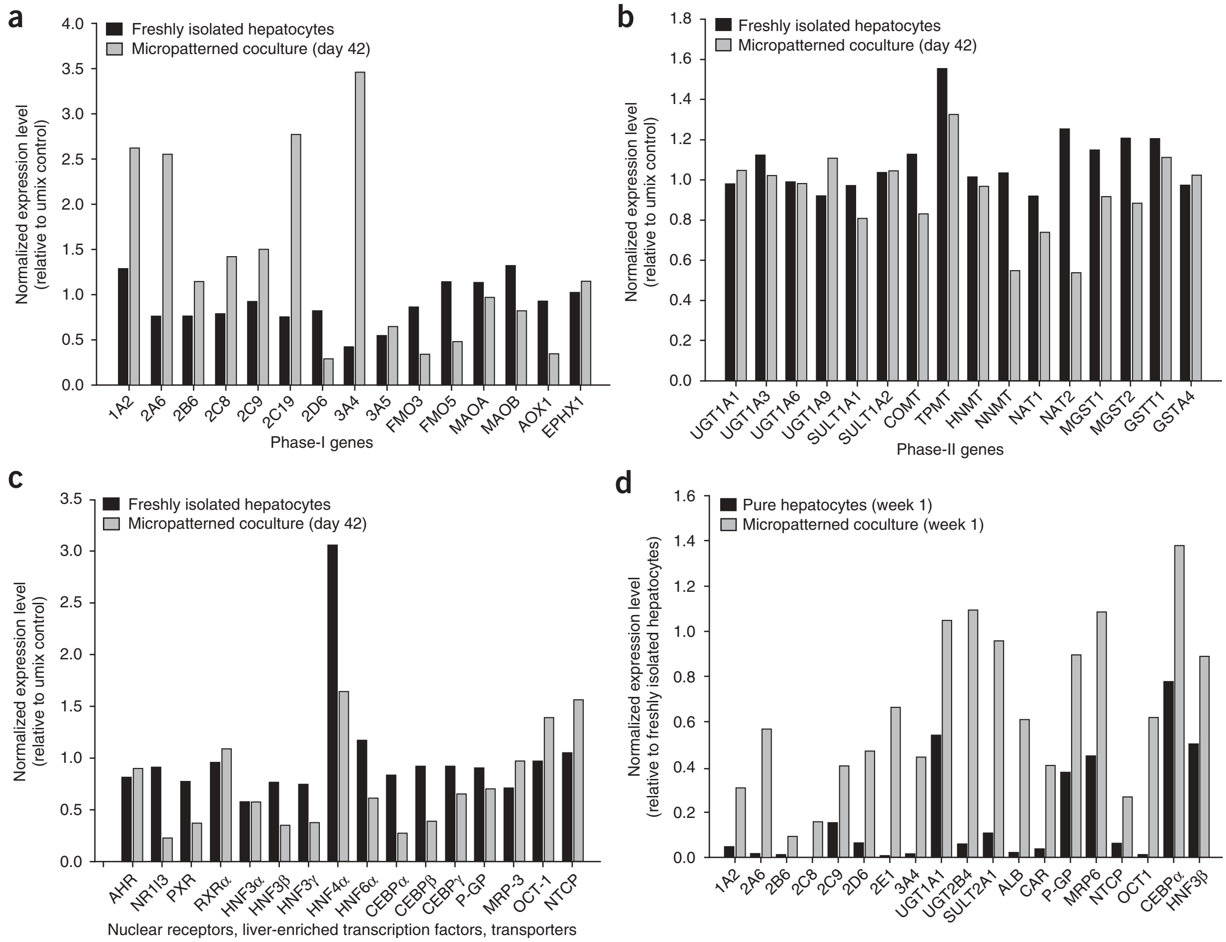

Figure 3 Gene expression profiling of hepatocytes in microscale liver cultures. (**a**) Quantitative comparison of phase I (i.e. CYP450, FMO) mRNA in hepatocytes from micropatterned cocultures (day 42) to mRNA in freshly isolated hepatocytes in suspension (day 0). All data was normalized to gene expression levels in a fresh, universal mixture of all cell types of the liver (umix, expression level of 1). FMO, flavin containing monooxygenase; MAO, monoamine oxidase; AOX1, aldehyde oxidase; EPHX1, epoxide hydrolase 1. (**b**) Quantitative comparison as in 'b', except that various Phase II genes are displayed. UGT, UDP glycosyltransferase; SULT, sulfotransferase; COMT, catechol-*O*-methyltransferase; TPMT, thiopurine *S*-methyltransferase; HNMT, histamine N-methyltransferase; NNMT, nicotinamide N-methyltransferase, NAT, N-acetyltransferase; GST, glutathione S-transferase; MGST, microsomal glutathione S-transferase. (**c**) Quantitative comparison as in 'a', except that various liver-specific genes (nuclear receptors, liver-enriched transcription factors, transporter genes) are displayed. AHR, aryl hydrocarbon receptor; NR1I3, nuclear receptor subfamily 1, group I, member 3 (also known as constitutive androstane receptor or CAR); PXR, pregnane X receptor; RXR, retinoid X receptor; HNF, hepatocyte nuclear factor; CEBP, CCAAT/enhancer binding protein; P-GP, P-glycoprotein; MRP3, multi-drug resistance protein 3; OCT, organic cation transporter; NTCP, sodium-dependent bile acid transporter. (**d**) Comparison of expression levels of various liver-specific transcripts in three models, which include: freshly isolated hepatocytes in suspension, pure hepatocytes 1 week after plating, and hepatocytes purified from 1 week old micropatterned cocultures. ALB, Albumin. All data was normalized to gene expression intensities in freshly isolated hepatocytes in suspension.

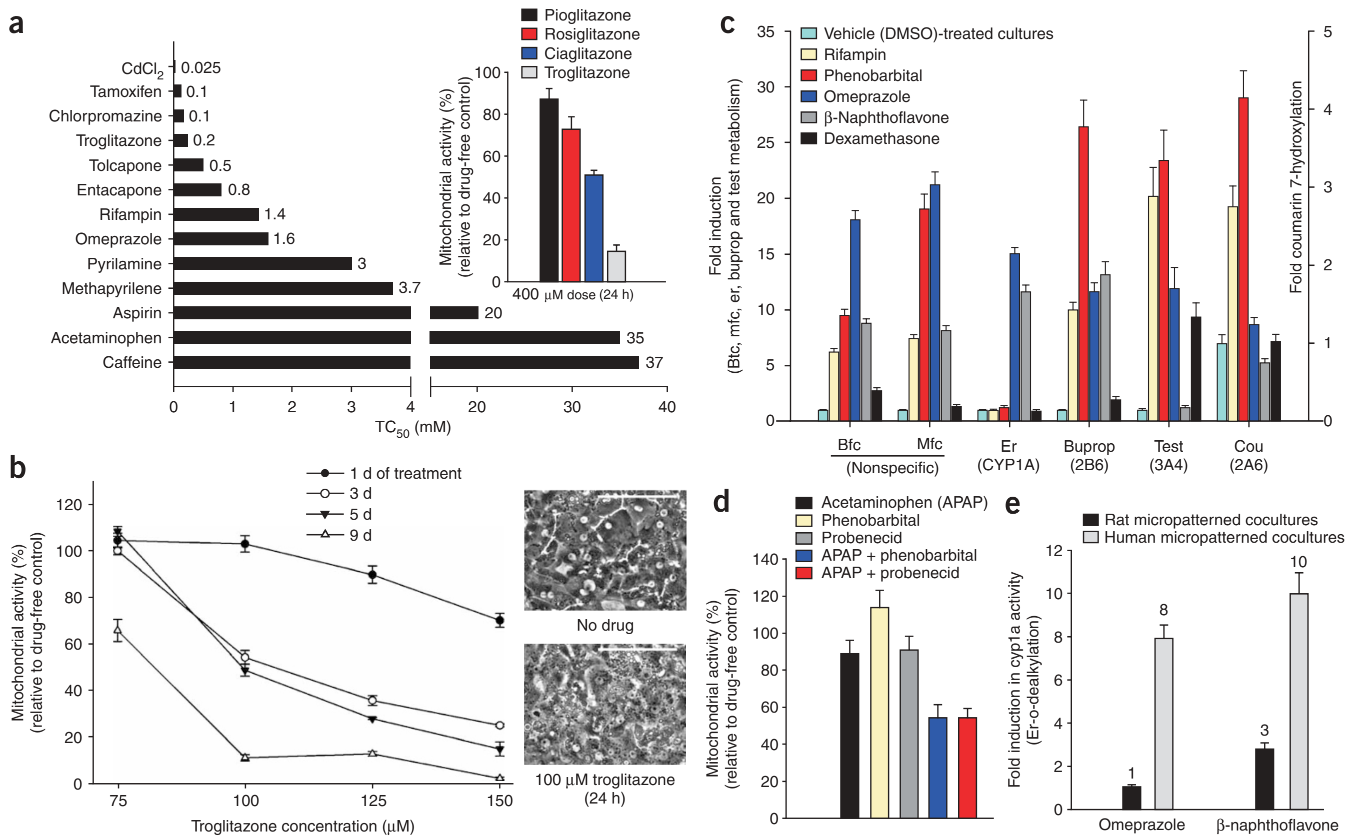

Figure 4 Utility of microscale liver cultures for screening of hepatotoxicity and drug interactions. (**a**) Rank ordering of a panel of compounds including several known hepatotoxins by TC_{50}, defined as the toxic concentration of drug which produces 50% decrease in mitochondrial activity after 24 h of exposure to 1- to 2-week-old micropatterned cocultures (acute toxicity). Mitochondrial toxicity was evaluated using the MTT assay (see Methods for details). Inset classifies relative toxicity of structurally-related PPARγ agonists in the thiazolidinediones class (24 h exposure at 400 μM). All data were normalized to a vehicle-only control. (**b**) Time and dose-dependent chronic toxicity of Troglitazone in micropatterned cocultures (2-3 week old). Cultures were dosed repeatedly every 48 h. All data was normalized to mitochondrial activity in untreated cultures (100% activity). Phase contrast micrographs show human hepatocyte morphology under untreated conditions and after treatment with 100 μM of Troglitazone for 24 h (scale bars are 100 μm). (**c**) Induction of CYP450 activity in micropatterned cocultures via prototypic clinical inducers. Cultures were treated for 3-4 d with inducers before incubation with fluorometric or conventional CYP450 substrates. All data was normalized to vehicle-only controls (fold change of 1). Mfc, 7-methoxy-4-trifluoromethylcoumarin; Bfc, 7-benzyloxy-4-trifluoromethylcoumarin; Test, Testosterone; Er, Ethoxy-resorufin; Bupro, Bupropion HCL; Cou, Coumarin. (**d**) Increase in acetaminophen (APAP) toxicity to 2 week old micropatterned cocultures due to drug interactions. CYP450s were induced in micropatterned cocultures with phenobarbital or glucuronidation was blocked with probenecid before administration of acetaminophen for 24 h. (**e**) Species-specific induction of CYP1A isoforms in micropatterned cocultures created using either primary rat or human hepatocytes. Data were normalized to vehicle-only controls. All error bars represent s.e.m. ($n = 3$).

by microscopy at concentrations lower than those required for cell death.

Modulation of CYP450s underlies drug interactions that can lead to serious pharmacological or toxicological consequences. We demonstrated CYP450 induction in micropatterned cocultures using clinical inducers and prototypic substrates (**Fig. 4c**). Induction profiles in micropatterned cocultures correlated well with the literature[12,17]. For instance, CYP1A was strongly induced (over tenfold) in micropatterned cocultures only upon incubation with AhR (aryl-hydrocarbon receptor) activators, omeprazole and β-naphthoflavone. On the other hand, CYP2A6 was induced strongly (over threefold) only by pregnane X receptor (PXR) activator, rifampin and the PXR/constitutive androstane receptor (CAR) activator phenobarbital. Modulation of CYP450s depends on both the dose and time of exposure to compounds. β-Naphthoflavone induced CYP1A2 activity[17] in a dose- and time-dependent manner in micropatterned cocultures, whereas methoxsalen (Oxsoralen, Uvadex) showed dose-dependent CYP2A6 inhibition[13] (**Supplementary Fig. 3**). To demonstrate the utility of our technology for evaluating drug interactions using toxicity as an endpoint, we used acetaminophen, an analgesic that undergoes CYP450-mediated conversion to a toxic metabolite and phase II-mediated detoxification[3]. Micropatterned cocultures were treated with either phenobarbital to induce CYP450s[17] or probenecid (Benemid, Probalan) to inhibit glucuronidation[22]. Further incubation of cultures with acetaminophen led to increased toxicity over that of controls (**Fig. 4d**), which is consistent with clinical findings[22,23]. Lastly, we demonstrated species-specific differences by comparing omeprazole (Prilosec)- and β-naphthoflavone-mediated CYP1A induction in cultures of human or rat hepatocytes[12,17] (**Fig. 4e**).

Our approach allows us to surround hepatocyte colonies with various liver- or nonliver-derived stroma[6,24] to create liver models with specific heterotypic interactions. We chose 3T3-J2 fibroblasts because of ready availability, ease of propagation, lack of liver-specific gene expression and induction of high levels of liver-specific functions in hepatocytes[16]. We also cocultivated micropatterned human hepatocytes with the nonparenchymal fraction of the human liver and observed stabilization of hepatic functions, although not to similar levels or duration as in cocultures with 3T3 fibroblasts (data not shown). Micropatterned clusters of human hepatocytes outperformed their randomly distributed counterparts by several-fold (**Supplementary Fig. 1**), consistent with reports that confluent cultures have higher hepatic functions than sparse ones, partly because of cadherin interactions[10]. Introduction of stroma further enhanced hepatocyte functions and longevity of the hepatocytes. Thus, our system uses an order-of-magnitude fewer hepatocytes and maintains phenotypic functions for several more weeks than conventional cultures in similar multiwell formats. Furthermore, we observed induction of liver-specific functions in micropatterned cocultures created using fresh hepatocytes from donors of different age groups, genders and medical histories (**Supplementary Table 1** online). Because the availability of fresh cells is limited, we also cultured cryopreserved human hepatocytes into our system (**Supplementary Fig. 4** online).

Conventional culture models expose hepatocytes to Matrigel and/or collagen-I gels. When used with near-confluent monolayers, these models allow better retention of hepatocyte cytoarchitecture and activity of specific CYP450s for a few more days ($\sim$1 week) compared with cultures on rigid collagen[10,12]. However, cell-cell contacts (homotypic and heterotypic) induce higher levels of phenotypic functions in human hepatocytes than extracellular matrix configuration or composition[6,9,10]. Here, we found that hepatic functions (albumin, urea, phase I/II) were better retained in micropatterned cocultures ($>$75% of fresh levels) compared with cultures using matrix gels ($<$22% of fresh levels, **Supplementary Fig. 5** online). Furthermore, micropatterned cocultures do not rely on fragile matrix gels, which can be difficult to scale down to 96- and 384-well formats.

Several other liver models using three-dimensional (3D) aggregates and/or continuous perfusion have been proposed[11,25–29]. Many of these strategies were developed for cell-based therapies where challenges are often around scale-up; however, a few have been scaled-down for drug screening[11,25,29,30]. Whereas 3D architecture is critical for therapeutic applications, limited *in situ* cell observation by conventional microscopy and nutrient transport limitations pose challenges for high-throughput screening of these models. Flowing medium can overcome nutrient transport limitations; however, inclusion of a flow circuit for each well introduces complexities in liquid handling and larger media volumes, requiring larger quantities of compounds. Thus, static two-dimensional monolayers are widely favored in industrial settings[10,12,17]. We have shown here that micropatterned cocultures maintain liver-specific functions well for several weeks and are compatible with robotic fluid handling, *in situ* microscopy and colorimetric/fluorescent plate-reader assays. This approach should be useful for ADME/Tox screening aimed at reducing costs, increasing the likelihood of clinical success and limiting human exposure to unsafe drugs.

METHODS

Micropatterning of collagen. Elastomeric PDMS stencil devices, consisting of thick-membranes ($\sim$300 μm) with through-holes (500 μm with 1,200-μm center-to-center spacing) at the bottom of each well of a 24-well mold were manufactured by Surface Logix, Inc. Stencil devices were first sealed (via gentle pressing) to tissue culture–treated polystyrene omnitrays (Nunc), then each well was incubated with a solution of type-I collagen in water (100 μg/ml) for 1 h at 37 °C. Purification of collagen from rat-tail tendons was previously described[16]. The excess collagen solution in each well was aspirated, the stencil was removed and a PDMS 'blank' (24-well mold without stencil membranes) was applied. Collagen-patterned polystyrene was stored dry at 4 °C for up to 4 weeks. In some cases, micropatterned collagen was fluorescently labeled by incubation (1 h at 23 °C) with Alexa Fluor 488 carboxylic acid, succinimidyl ester (Invitrogen) dissolved in PBS at 20 μg/ml. For experiments in **Supplementary Figure 1**, collagen was micropatterned in various dimensions on glass substrates using conventional photolithographic techniques, as described previously[6].

Hepatocyte isolation and culture. Primary rat hepatocytes were isolated from 2- to 3-month old adult female Lewis rats (Charles River Laboratories) weighing 180–200 g. Detailed procedures for rat hepatocyte isolation and purification were previously described[16]. Routinely, 200–300 million cells were isolated with 85–95% viability and $>$99% purity. Hepatocyte culture medium consisted of DMEM with high glucose, 10% (vol/vol) FBS, 0.5 U/ml insulin, 7 ng/ml glucagon, 7.5 μg/ml hydrocortisone and 1% (vol/vol) penicillin-streptomycin. Primary human hepatocytes were purchased in suspension from vendors permitted to sell products derived from human organs procured in the United States by federally designated Organ Procurement Organizations. Hepatocyte vendors included: Celsis *In vitro* Technologies, Lonza, BD-Gentest, ADMET Technologies, CellzDirect and Tissue Transformation Technologies (now part of BD-Gentest). All work was done with the approval of COUHES (Committee on use of human experimental subjects). Upon receipt, human hepatocytes were pelleted by centrifugation at 50*g* for 5 min (4 °C). The supernatant was discarded, cells were resuspended in hepatocyte culture medium, and viability was assessed using Trypan blue exclusion (typically 70–90%). Liver-derived nonparenchymal cells, as judged by their size ($<$10 μm diameter) and morphology (nonpolygonal), were consistently found to be less than 1% in these preparations.

Hepatocyte-fibroblast cocultures. To create micropatterned cocultures, we first produced a hepatocyte pattern by seeding hepatocytes on collagen-patterned substrates that mediate selective cell adhesion. The cells were washed with medium 2–3 h later to remove unattached cells ($\sim$10,000 adherent hepatocytes in 37 collagen-coated islands) and incubated in hepatocyte medium overnight. 3T3-J2 fibroblasts were seeded (30,000 total) in fibroblast medium 12–24 h later to create cocultures. Fibroblast-to-hepatocyte ratio was estimated by a hemocytometer to be 4:1, once the fibroblasts reached confluency in cocultures and their growth was contact inhibited. Fibroblast culture medium was replaced to hepatocyte culture medium 24 h after fibroblast seeding and subsequently replaced daily (300 μl per well in 24-well format). For randomly distributed cultures, hepatocytes were seeded on substrates (glass or polystyrene) with a uniform coating of collagen. In some cases, hepatocytes were fluorescently labeled through incubation (1 h at 37 °C) with Calcein-AM (Invitrogen) dissolved in culture medium at 5 μg/ml. Fibroblasts were fluorescently labeled with CellTracker (Orange CMTMR, Invitrogen) as per manufacturer's instructions.

Biochemical assays. Spent medium was stored at –20 °C. Urea concentration was assayed using a colorimetric endpoint assay using diacetylmonoxime with acid and heat (Stanbio Labs). Albumin content was measured using enzyme-linked immunosorbent assays (MP Biomedicals) with horseradish peroxidase detection and 3,3′,5,5′-tetramethylbenzidine (TMB, Fitzgerald Industries) as a substrate[16].

Cytochrome-P450 induction. Stock solutions of prototypic CYP450 inducers (Sigma) were made in dimethylsulfoxide (DMSO), except for phenobarbital, which was dissolved in water. Cultures were treated with inducers (rifampin, β-naphthoflavone, dexamethasone at 25 μM each, omeprazole at 50 μM, and phenobarbital at 1 mM) dissolved in hepatocyte culture medium for 3–4 d. Control cultures were treated with vehicle (DMSO) alone for calculations of fold induction. To enable comparisons across inducers, we kept DMSO levels constant at 0.1% (vol/vol) for all conditions.

Toxicity assays. Cultures were incubated with various concentrations of compounds dissolved in culture medium for 24 h (acute toxicity) or extended time periods (chronic toxicity, 1–9 d). Cell viability was subsequently measured by the MTT (3-(4,5-dimethylthiazol-2-yl)-2,5-diphenyl tetrazolium bromide; Sigma) assay, which involves cleavage of the tetrazolium ring by mitochondrial dehydrogenase enzymes to form a purple precipitate. MTT was added to cells in DMEM without phenol red at a concentration of 0.5 mg/ml. After an incubation time of 1 h, the purple precipitate was dissolved in a 1:1 solution of DMSO and isopropanol. The absorbance of the solution was measured at 570 nm (SpectraMax spectrophotometer, Molecular Devices).

Statistical analysis. Experiments were repeated at least 2–3 times with duplicate or triplicate samples for each condition. Data from representative experiments are presented, whereas similar trends were seen in multiple trials. All error bars represent s.e.m.

Note: Supplementary information is available on the Nature Biotechnology website.

ACKNOWLEDGMENTS

We are grateful to Emanuele Ostuni and Surface Logix, Inc. for design and fabrication of the PDMS stencils, Howard Green for providing 3T3-J2 fibroblasts, Jennifer Koh for assistance with pilot studies, David Eddington for assistance with microfabrication, Taylor Sittler for helpful discussions regarding compound selection, Elise Liu for assistance with biochemical assays and Sandra March for assistance with RNA isolation. Funding was generously provided by a National Science Foundation (NSF) graduate fellowship (S.R.K.), NSF CAREER, National Institutes of Health National Institute of Diabetes and Digestive and Kidney Diseases, Deshpande Center at MIT, the David and Lucile Packard Foundation, the Massachusetts Technology Transfer Center, and the Center for Environmental Health Sciences at MIT.

AUTHOR CONTRIBUTIONS

S.R.K. designed and performed the experiments, analyzed the data and wrote the manuscript. S.N.B. designed the experiments, analyzed the data and wrote the manuscript.

COMPETING INTERESTS STATEMENT

The authors declare competing financial interests: details accompany the full-text HTML version of the paper at http://www.nature.com/naturebiotechnology/.

Published online at http://www.nature.com/naturebiotechnology/
Reprints and permissions information is available online at http://npg.nature.com/reprintsandpermissions

1. Voldman, J., Gray, M.L. & Schmidt, M.A. Microfabrication in biology and medicine. *Annu. Rev. Biomed. Eng.* **1**, 401–425 (1999).
2. Khetani, S.R. & Bhatia, S.N. Engineering tissues for in vitro applications. *Curr. Opin. Biotechnol.* **17**, 524–531 (2006).
3. Kaplowitz, N. Idiosyncratic drug hepatotoxicity. *Nat. Rev. Drug Discov.* **4**, 489–499 (2005).
4. Viravaidya, K. & Shuler, M.L. Incorporation of 3T3–L1 cells to mimic bioaccumulation in a microscale cell culture analog device for toxicity studies. *Biotechnol. Prog.* **20**, 590–597 (2004).
5. Chen, C.S., Mrksich, M., Huang, S., Whitesides, G.M. & Ingber, D.E. Geometric control of cell life and death. *Science* **276**, 1425–1428 (1997).
6. Bhatia, S.N., Balis, U.J., Yarmush, M.L. & Toner, M. Effect of cell-cell interactions in preservation of cellular phenotype: cocultivation of hepatocytes and nonparenchymal cells. *FASEB J.* **13**, 1883–1900 (1999).
7. Pritchard, J.F. *et al.* Making better drugs: Decision gates in non-clinical drug development. *Nat. Rev. Drug Discov.* **2**, 542–553 (2003).
8. Gebhardt, R. *et al.* New hepatocyte in vitro systems for drug metabolism: metabolic capacity and recommendations for application in basic research and drug development, standard operation procedures. *Drug Metab. Rev.* **35**, 145–213 (2003).
9. Guillouzo, A. Liver cell models in in vitro toxicology. *Environ. Health Perspect.* **106** Suppl 2, 511–532 (1998).
10. LeCluyse, E.L. Human hepatocyte culture systems for the in vitro evaluation of cytochrome P450 expression and regulation. *Eur. J. Pharm. Sci.* **13**, 343–368 (2001).
11. Sivaraman, A. *et al.* A microscale in vitro physiological model of the liver: predictive screens for drug metabolism and enzyme induction. *Curr. Drug Metab.* **6**, 569–591 (2005).
12. Hewitt, N.J. *et al.* Primary hepatocytes: current understanding of the regulation of metabolic enzymes and transporter proteins, and pharmaceutical practice for the use of hepatocytes in metabolism, enzyme induction, transporter, clearance, and hepatotoxicity studies. *Drug Metab. Rev.* **39**, 159–234 (2007).
13. Donato, M.T., Jimenez, N., Castell, J.V. & Gomez-Lechon, M.J. Fluorescence-based assays for screening nine cytochrome P450 (P450) activities in intact cells expressing individual human P450 enzymes. *Drug Metab. Dispos.* **32**, 699–706 (2004).
14. Wilkening, S., Stahl, F. & Bader, A. Comparison of primary human hepatocytes and hepatoma cell line Hepg2 with regard to their biotransformation properties. *Drug Metab. Dispos.* **31**, 1035–1042 (2003).
15. Whitesides, G.M., Ostuni, E., Takayama, S., Jiang, X. & Ingber, D.E. Soft lithography in biology and biochemistry. *Annu. Rev. Biomed. Eng.* **3**, 335–373 (2001).
16. Khetani, S.R., Szulgit, G., Del Rio, J.A., Barlow, C. & Bhatia, S.N. Exploring interactions between rat hepatocytes and nonparenchymal cells using gene expression profiling. *Hepatology* **40**, 545–554 (2004).
17. Madan, A. *et al.* Effects of prototypical microsomal enzyme inducers on cytochrome P450 expression in cultured human hepatocytes. *Drug Metab. Dispos.* **31**, 421–431 (2003).
18. Waring, J.F. *et al.* Isolated human hepatocytes in culture display markedly different gene expression patterns depending on attachment status. *Toxicol. In Vitro* **17**, 693–701 (2003).
19. Richert, L. *et al.* Gene expression in human hepatocytes in suspension after isolation is similar to the liver of origin, is not affected by hepatocyte cold storage and cryopreservation, but is strongly changed after hepatocyte plating. *Drug Metab. Dispos.* **34**, 870–879 (2006).
20. Rodriguez-Antona, C., Donato, M.T., Pareja, E., Gomez-Lechon, M.J. & Castell, J.V. Cytochrome P-450 mRNA expression in human liver and its relationship with enzyme activity. *Arch. Biochem. Biophys.* **393**, 308–315 (2001).
21. Isley, W.L. Hepatotoxicity of thiazolidinediones. *Expert Opin. Drug Saf.* **2**, 581–586 (2003).
22. Kamali, F. The effect of probenecid on paracetamol metabolism and pharmacokinetics. *Eur. J. Clin. Pharmacol.* **45**, 551–553 (1993).
23. Pirotte, J.H. Apparent potentiation of hepatotoxicity from small doses of acetaminophen by phenobarbital. *Ann. Intern. Med.* **101**, 403 (1984).
24. Corlu, A. *et al.* The coculture: a system for studying the regulation of liver differentiation/proliferation activity and its control. *Cell Biol. Toxicol.* **13**, 235–242 (1997).
25. Eschbach, E. *et al.* Microstructured scaffolds for liver tissue cultures of high cell density: morphological and biochemical characterization of tissue aggregates. *J. Cell. Biochem.* **95**, 243–255 (2005).
26. Allen, J.W., Hassanein, T. & Bhatia, S.N. Advances in bioartificial liver devices. *Hepatology* **34**, 447–455 (2001).
27. Naughton, B.A., Sibanda, B., Weintraub, J.P., San Roman, J. & Kamali, V. A stereotypic, transplantable liver tissue-culture system. *Appl. Biochem. Biotechnol.* **54**, 65–91 (1995).
28. Kaihara, S. *et al.* Survival and function of rat hepatocytes cocultured with nonparenchymal cells or sinusoidal endothelial cells on biodegradable polymers under flow conditions. *J. Pediatr. Surg.* **35**, 1287–1290 (2000).
29. Kane, B.J., Zinner, M.J., Yarmush, M.L. & Toner, M. Liver-specific functional studies in a microfluidic array of primary Mammalian hepatocytes. *Anal. Chem.* **78**, 4291–4298 (2006).
30. Zeilinger, K. *et al.* Three-dimensional co-culture of primary human liver cells in bioreactors for in vitro drug studies: effects of the initial cell quality on the long-term maintenance of hepatocyte-specific functions. *Altern. Lab. Anim.* **30**, 525–538 (2002).